Brain Structure and Function (2026) 231:104
https://doi.org/10.1007/s00429-026-03160-2

ORIGINAL ARTICLE

Associations between READ1 deletion, reading proficiency, and white matter network organisation in children with and without developmental dyslexia

Marina Di Stefano[1,2] · Sara Mascheretti[3,4] · Valentina Lampis[3,4] · Matteo Di Segni[4] · Chiara Mauri[4] · Francesca Maccarone[1,5] · Filippo Arrigoni[6] · Denis Peruzzo[1]

Received: 27 February 2026 / Accepted: 7 July 2026

Abstract

Developmental dyslexia (DD) is a common neurodevelopmental disorder, whose causes lie in genetic and neurobiological underpinnings. *DCDC2* is one of the most replicated candidate genes underlying the etiology of reading (dis)abilities and has been associated with neural migration patterns. Although a deletion within intron 2 of the *DCDC2*, encompassing the entire READ1 (hereafter READ1d), has been reported to be linked to structural and functional brain alterations, its impact on white matter connectivity was not fully explored. In this study, we investigated how the READ1d influences white matter network organization and its relationship with reading ability. Seventy-four children (47 M/27 F, age in months: 161 ± 22) with/without a diagnosis of DD and with/without READ1d underwent diffusion MRI, from which graph-theoretical analysis was performed. Statistical analyses tested the effects of READ1d, reading proficiency, and their interaction, with age, sex, IQ, and attention scores included as covariates. Regardless of reading performance, subjects with READ1d showed nominally significant lower global efficiency, local efficiency, and clustering coefficient compared to subjects without READ1d, with consistent effect directions across metrics; the nodal analysis revealed a significant effect of READ1d on a network spanning lateral, occipital and frontal cortex. Reading performance was associated with a network in the left occipital-temporal cortex at the level of nodal degree and a scattered bilateral network for local efficiency. These findings are consistent with an association between READ1d carrier status and subtle but widespread differences in network integration and nodal connectivity, observed regardless of reading performance, and offer a framework for future multimodal investigations into the genetic architecture of reading disorders.

Keywords Developmental dyslexia · Diffusion MRI · Structural connectivity · Genetics

✉ Denis Peruzzo
denis.peruzzo@lanostrafamiglia.it

Marina Di Stefano
marina.distefano@lanostrafamiglia.it

Sara Mascheretti
sara.mascheretti@lanostrafamiglia.it

Valentina Lampis
valentina.lampis@lanostrafamiglia.it

Matteo Di Segni
matteo.disegni@lanostrafamiglia.it

Chiara Mauri
chiara.mauri@lanostrafamiglia.it

Francesca Maccarone
francesca.maccarone@lanostrafamiglia.it

Filippo Arrigoni
filippo.arrigoni@asst-fbf-sacco.it

[1] NeuroImaging Laboratory, Scientific Institute IRCCS Eugenio Medea, Lecco, Italy

[2] Division Imaging and Oncology, Image Sciences Institute, University Medical Center Utrecht, Utrecht, The Netherlands

[3] Department of Brain and Behavioral Sciences, University of Pavia, Pavia, Italy

[4] Child Psychopathology Unit, Scientific Institute IRCCS Eugenio Medea, Lecco, Italy

[5] University of Milano-Bicocca, Milan, Italy

[6] Department of Radiology and Neuroradiology, Children's Hospital V. Buzzi, Milan, Italy

Published online: 20 July 2026

Abbreviations

DD	Developmental dyslexia
DK	Desikan killiany
GE	Global efficiency
LE	Local efficiency
CC	Clustering coefficient
SW	Small-worldness
ND	Nodal degree
NE	Nodal local efficiency
BC	Betweenness centrality
SPC	Statistical parametric connectome
GLM	General linear model

Introduction

Developmental dyslexia (DD) is one of the most common heritable neurodevelopmental disorders in school-aged children (~7%-15%, Peterson and Pennington 2015) characterized by reading difficulties that are not caused by intellectual disability, limited access to education, sensory or neurological impairments (Lyon et al. 2003). Over the past decades neuroimaging studies have tried to elucidate the neural underpinnings of DD, from both functional and structural perspective (Galaburda 1993; Mascheretti et al. 2017; Landi and Perdue 2019). In particular, diffusion-weighted magnetic resonance imaging (dMRI) studies have repeatedly highlighted the role of white matter (WM) integrity and structural connectivity in DD (Beaulieu et al. 2005; Boets et al. 2013; Deutsch et al. 2005; Rimrodt et al. 2010; Vandermosten et al. 2012; Lou et al. 2019; Zhao et al. 2024).

By sampling water molecules diffusion along multiple gradient directions, dMRI allows to model their local displacement within each voxel, providing indirect but sensitive markers of WM organization (Jelescu and Budde 2017). Diffusion tensor imaging (DTI) has historically been the preferential choice for quantifying WM integrity by providing metrics assessing the average rate (mean diffusivity, MD) and orientation coherence (fractional anisotropy, FA) of diffusion (Basser et al. 1994). Following this approach, lower FA has been reported in long association tracts such as the arcuate fasciculus (AF), inferior fronto-occipital fasciculus (IFOF), inferior longitudinal fasciculus (ILF), and across the corpus callosum (CC) with subjects with DD (Vandermosten et al. 2012; Mascheretti et al. 2017; Landi and Perdue 2019). Although powerful for testing hypotheses about specific, predefined tracts, this approach requires the a priori selection of tracts of interest and, while it can characterize local microstructural properties, it cannot capture network-level organization (Farahani et al. 2019).

Besides voxel-wise metrics, the diffusion profile within each voxel allows to infer the orientation of WM fibers and to get an estimate of their 3D pathways (Behrens et al. 2007; Maier-Hein et al. 2017; Tournier et al. 2019). These reconstructions, or tractograms, can provide a model representing the global fiber architecture of the brain by defining quantitative information on the structural connections between brain regions through structural connectivity matrices (i.e., connectomes; Škoch et al. 2022). Graph-theoretical analysis of the connectomes quantifies network integration and segregation beyond single-tract measures. Unlike voxel-wise or tract-specific DTI approaches, graph-theoretical analysis captures emergent topological properties of the entire structural connectome, such as global integration and network organisation, that cannot be reduced to local microstructural measures. This could make it particularly appropriate for investigating the network-level consequences of genetic variants that affect brain development. Using this approach, Lou and colleagues (2019) identified decreased streamlines within a network connecting the left-occipital-temporal cortex and temporo-parietal cortex in children with DD. The authors speculated that the group differences between children with DD and typical readers (TRs) found in the local temporo-parietal network may have genetic basis (Lou et al. 2019). However, the extent to which genetic risk modulates whole-brain structural topology in DD remains largely unexplored.

DD is a highly heritable complex trait, with heritability estimates ranging from 0.18 to 0.72 (Andreola et al. 2021). Although they have not been replicated in recent genome-wide association studies, molecular genetics has identified several candidate genes for reading (dis)ability (Peterson and Pennington 2015; Mascheretti et al. 2017; Scerri and Schulte-Körne 2010) which are involved in key neurodevelopmental processes such as neuronal migration, neurite outgrowth, cortical morphogenesis, and ciliary function (Lampis et al. 2021). Among these genes, *DCDC2* has been associated with reading skills in both general population and clinical samples (Scerri and Schulte-Körne 2010; Carrion-Castillo et al. 2013; Zhong et al. 2013; Mascheretti et al. 2017; Landi and Perdue 2019). As emerged from animal studies, it encodes a protein with two DCX domains critical for neuronal migration, cortical organization, and ciliary function (Lampis et al. 2021). Its partial or total inactivation has been linked to altered neuronal excitability and temporal precision, potentially impairing visual information processing (Meng et al. 2005) and contributing to reading-related behavioral deficits (Lampis et al. 2021). Meng et al. (2005) reported a 168-base pair purine-rich region in the intron 2 of the DCDC2 gene harboring a highly polymorphic, short-tandem repeat (BV677278). Given its evolutionary conservation and the presence of 131 potential binding sites for transcription factors, this non-coding segment is thought to have a significant regulatory function. Meng et al. (2011)

demonstrated through in vitro testing that specific alleles act as enhancers for gene transcription. Powers et al. (2013) identified transcription factor ETV6 as a BV677278-binding protein and confirmed BV677278 as a regulatory element, named "regulatory element associated with dyslexia 1″ (READ1). Although negative findings have recently been described (Powers et al. 2016; Scerri et al. 2017), a naturally occurring deletion encompassing READ1 (hereafter, READ1d) has been consistently associated with DD and DD-related phenotypes (Brkanac et al. 2007; Harold et al. 2006; Marino et al. 2012; Powers et al. 2016; Wilcke et al. 2009), deficits in visual motion perception (Meng et al. 2011; Marino et al. 2012; Cicchini et al. 2015), and altered functional activations (Cope et al. 2012; Mascheretti et al. 2024).

By implementing DTI models, previous studies have pointed DCDC2 markers (Lind et al. 2010; Darki et al. 2012, 2014) and READ1d (Perani et al. 2021; Marino et al. 2014) affecting WM integrity in regions involved in reading (dis)ability. These tract-level analyses, however, provide only a partial picture of how READ1d shapes the broader architecture of structural brain networks. Taken together with previous data, our study investigates whether READ1d may affect structural connectivity as reading proficiency changes. To address this prediction, we applied advanced tractography to build subject-level connectomes and compute global and local network metrics in subjects with DD with/without READ1d ($n=36$) and in TRs with/without READ1d ($n=38$). To the best of our knowledge, this is the first study that systematically investigated the genetic origins of WM network organization and how this relationship can be affected by different levels of reading proficiency.

Materials and methods

The protocol was approved by the Scientific Review Board and the Ethical Committee of the Scientific Institute IRCCS Eugenio Medea.

Sample

The study drew DD subjects (American Psychiatric Association 2006) from a sample previously genotyped for READ1d ($N=930$) (Riva et al. 2019). Inclusion criteria for the original genetic study required: (1) a reading accuracy or speed z-score ≤ -2.00 on at least one standardised test, including text reading, reading of single unrelated words, or reading of pronounceable pseudowords (Cornoldi 1995; Cornoldi and Colpo 1998; Sartori et al. 1995; Arina et al. 2013); (2) a mean weighted score ≥ 7 ($z \geq -1.00$) on the vocabulary and block design subtests of the WISC-III (Wechsler 2006); and (3) absence of neuropsychiatric, neurological, or sensory disorders. Within this cohort, 114 participants carried READ1d (1 homozygous, 113 heterozygous; allelic frequency = 0.078) and 816 did not. Given the population-level imbalance in READ1d frequency, all parents of READ1d carriers were contacted, and non-carriers were randomly selected to form groups of approximately equal size, subject to logistical constraints. TR participants were recruited through two independent channels. In the first recruitment scheme, 124 children aged 10–18 with no MRI contraindications, no neuropsychiatric, neurological, or sensory disorders, and normal or corrected-to-normal vision were contacted through word-of-mouth outreach among students attending middle and high schools in the Milan and Lecco area. Parental written informed consent for DNA collection via mouthwash sample was obtained from all 124 participants. Genotyping identified 15 READ1d carriers (all heterozygous; allelic frequency = 0.069) and 109 non-carriers. In the second recruitment scheme, participants were drawn from a community-based cohort of Italian children previously recruited for a larger study investigating the effects of genetic and environmental risk factors on behavioural, cognitive, and linguistic development (Riva et al. 2015). For the present study, a subsample of 235 children from one of five school districts involved in the original study was considered. Genotyping data for READ1d were available for 194 of these 235 participants, yielding 43 READ1d carriers (1 homozygous, 42 heterozygous) and 151 non-carriers. The allelic frequency of READ1d in this subsample did not differ significantly from that observed in the remaining four school districts (data available upon request).

All participants were included if: (i) belonging to Caucasian families who were at least first-generation native Italian speakers, to ensure linguistic and normative comparability of the reading assessments; (ii) having no certified neurological, neurodevelopmental, visual, hearing, intellectual or motor disabilities; (iii) having written informed consent signed by both parents; (iv) being 10–18 years old; (v) had no contraindications to MRI.

Neuropsychological assessment

Both children with DD and TRs underwent the following neuropsychological assessments:

(1) IQ. It was estimated by the vocabulary and block design subscales of the WISC-III (Wechsler 2006); the test evaluates a child's global intellectual capacity through a variety of subtests that measure specific mental abilities such as abstract reasoning, memory, and information processing.

(2) Reading. It was assessed through three tests: text, single unrelated words and pseudo-words reading tests (Cornoldi 1995; Cornoldi and Colpo 1998). The single words/pseudo-words reading test was evaluated with the DDE-2: Batteria per la Valutazione della Dislessia e Disortografia Evolutiva-2 (Sartori et al. 2007), which measures reading speed and accuracy (number of errors) for lists of single words (4 lists of 24 items) and pseudo-words (3 lists of 16 items). Grade-based norms are available from second grade of primary school through the final year of middle school. Reliability was >0.70 for speed (both single words and pseudo-words) and >0.55 for accuracy (both single words and pseudo-words); concurrent validity was above >0.70 (Sartori et al. 2007). Text reading was assessed with the Prove di Rapidità e Correttezza nella Lettura del Gruppo MT (Cornoldi and Carretti 2016), which evaluates reading speed and accuracy on meaningful passages of increasing complexity, with grade-specific norms. Test-retest reliability was >0.80 and >0.70 for speed and accuracy, respectively (Cornoldi and Carretti 2016. Speed (time in seconds) (Tressoldi et al. 2012) and accuracy (number of errors) were recorded and converted in z-scores (Sartori et al. 2007).

(3) Since bivariate correlations (r) across reading tasks were substantial (Mascheretti et al. 2024), a single reading score was obtained by averaging the z-scores from the six reading parameters (hereafter, Mean Reading);

(4) ADHD traits. They were assessed by the Conners' Parent Rating Scales–Revised: Long version (CPRS-R: L) (Conners 1989; Conners et al. 1998; Nobile et al. 2007) which rates childhood behavioral problems in subjects aged 3–17 years old (Conners et al. 1998). The CPRS-R: L consists of 80 items rated on a 4-point Likert scale (from "0 = never or rarely observed" to "3 = very often"), and yields 14 subscales. The scores were transformed into age- and gender-adjusted T-scores for analyses. Higher scores (T-score ≥ 65) indicate more problems. For the current purpose, only the DSM-IV Inattention subscale (DSM-IV-I) was considered, given that the DD–ADHD comorbidity is consistently more pronounced for inattention than for hyperactivity/impulsivity, both phenotypically (Plourde et al. 2015; Rosenberg et al. 2012) and at the genetic level (Greven et al. 2011, 2012; Paloyelis et al. 2010; Willcutt et al. 2010).

Socioeconomic status was defined on grounds of parental occupation which was scored according to the Hollingshead nine-points scale, whereby a score ranging from 10 to 90 was assigned to each parental job, and the higher of the two scores was used when both parents were employed (Hollingshead 1975).

MRI acquisition protocol

MRI data were acquired on a 3T Philips Achieva d-Stream scanner (Best, The Netherlands) with a 32-channel head coil. The MRI protocol included an anatomical T1-weighted (T1W) 3D Turbo Field Echo sequence as a subject morphological reference of MRI data (Field Of View (FOV) = 256 × 256 × 175 mm^3, voxel size 1 × 1 × 1 mm^3, repetition time=shortest (~8.1 ms), Time of Echo (TE)=shortest (~3.7 ms), Flip Angle (FA) = 8 deg.

dMRI data were acquired with an Echo Planar Imaging (EPI) sequence (FOV = 144 × 144 mm^2, voxel size = 1.7 × 1.7 mm^2, slice thickness = 2.5 mm, slice number = 39, repetition time = 2 s, TE = 80 ms, FA = 90 deg). The sequence included 36 volumes: 4 b0 volumes, and 32 directions at b = 2500 s/mm^2. Furthermore for 50/74 subjects, a sequence in the reversed-encoding direction was acquired with 2 b0 and 10 directions at b = 2500 s/mm^2. Groups did not differ significantly in the distribution of acquisition parameters (SynB0, $\chi^2 = 0.406$, $p = .939$; see Supplementary Materials Fig. S1). Head motion metrics were computed for all subjects and are reported in Supplementary Materials, Table S1. All metrics were within acceptable ranges for pediatric dMRI at b = 2500 s/mm^2; indeed subjects with unusable scans had been excluded prior to analysis.

T1-weighted preprocessing

T1-weighted (T1w) images were first corrected for intensity non-uniformities using the N4 bias field correction algorithm (Tustison et al. 2010). Following this, cortical and subcortical anatomical structures were segmented using the FreeSurfer image analysis suite (version 7.2; http://surfer.nmr.mgh.harvard.edu/), following the standard *recon-all* processing pipeline. Desikan Killiany (DK) atlas was provided for brain parcellations and then for connectome construction. It includes 34 cortical regions for each hemisphere (Desikan et al. 2006). To these we added 7 subcortical regions for each hemisphere, based on FreeSurfer segmentation (cerebellum, caudate, putamen, pallidum, hippocampus, amygdala, accumbens). This resulted in 82 parcels.

Diffusion MRI preprocessing

dMRI data were preprocessed using the MRtrix3 framework (Tournier et al. 2019; Tahedl et al. 2025). Preprocessing steps included denoising to reduce scanner and thermal noise; removal of Gibbs ringing artifacts; correction for motion and eddy-current-induced distortions. These latter steps were performed applying the typical correction procedure as implemented in MRtrix3 through the *dwipreproc* function, which exploits the double phase-encoding (PE)

acquisition. For the subjects lacking a double PE acquisition, EPI distortion correction was performed applying the Synb0-DisCo pipeline (Schilling et al. 2019). The algorithm generates an undistorted synthetic b0 image from the subject's T1w image via a deep learning model. This synthetic image, which simulates infinite bandwidth in the PE direction, was then paired with the real distorted b0 image and passed to FSL's TOPUP tool. TOPUP estimates a distortion field using the two b0 images, effectively bypassing the need for reverse-PE acquisitions. This approach has demonstrated anatomically accurate correction results comparable to standard reverse-PE methods (Schilling et al. 2019).

Bias field correction was applied to the diffusion data to remove residual low-frequency intensity inhomogeneities. A brain mask was then extracted for subsequent processing through *dwi2mask* function. Due to the single-shell acquisition scheme, Single-Shell 3-Tissue Constrained Spherical Deconvolution (SS3T-CSD) (Dhollander and Connelly 2019) was applied using MRtrix3Tissue (https://3Tissue.github.io), a fork of MRtrix3 (Tournier et al. 2019), to compute WM-like fiber orientation distributions (FODs) and isotropic signal components (GM- and CSF-like) for all voxels.

Tractography

Whole-brain probabilistic tractography was conducted using the iFOD2 algorithm (Second-order Integration over Fiber Orientation Distributions), in combination with Anatomically Constrained Tractography (ACT) based on 5-tissue-type (5TT) images. Standard MRtrix3 tracking parameters were used: step size = 0.2 mm, maximum angle = 60°, and FOD amplitude threshold = 0.1 (Smith et al. 2012).

To enhance anatomical plausibility, additional features included dynamic seeding, backtracking, and streamline cropping at the grey–white matter interface. The interface was derived from the MRtrix3 5-tissue segmentation of the T1-weighted image. To ensure that subcortical regions were also included, the first volume was modified to incorporate deep GM. For each subject, 20 million streamlines were generated. To mitigate known biases of CSD, we applied Spherical-deconvolution Informed Filtering of Tractograms (SIFT2) (Smith et al. 2015). Each tractogram was visually inspected to ensure anatomical plausibility after filtering.

Connectome construction

Connectome matrices were generated by mapping streamlines to cortical and subcortical regions defined by the DK parcellations. This resulted in symmetric 82×82 adjacency matrices for each subject. Raw edge weights represent the sum of streamline contributions between each parcel pair ($\Sigma\mu_k$ over all streamlines connecting parcels i and j), where each streamline weight μ_k is derived from the SIFT2 algorithm and reflects its contribution to the fibre orientation distribution fit. Volume scaling was applied by dividing each edge weight by the sum of the volumes of the two endpoint parcels, using subject-specific parcel volumes derived from each individual's parcellation (Tahedl, 2020; Tahedl et al. 2025). Following (Tahedl et al. 2025), and given the arbitrariness of thresholding approaches, fully weighted matrices including all non-zero edges were used.

Graph analysis

To assess network topology, both global and local graph metrics were extracted from weighted adjacency matrices using the Brain Connectivity Toolbox (Rubinov and Sporns 2010; https://sites.google.com/site/bctnet/).

Global metrics included:

- Global Efficiency (GE), defined as the mean inverse shortest path length between all node pairs, reflecting network integration;
- Local Efficiency (LE), defined as the average efficiency of local subgraphs, indicating robustness to node failure;
- Clustering Coefficient (CC), defined as the tendency of nodes to form tightly interconnected groups;
- Small-Worldness (SW), defined as the degree to which a network maintains high clustering and short path lengths relative to a random graph.

Local metrics (i.e. referred to nodes) included:

- Nodal Degree (ND), defined as the number of direct connections to a node;
- Nodal Local Efficiency (NE), defined as the efficiency of communication within a node's local neighborhood;
- Betweenness Centrality (BC), defined as the proportion of shortest paths passing through a node, reflecting its control over information flow.

Node abbreviations follow the Desikan-Killiany atlas labelling scheme and are listed in full in Fig. 2.

Statistical analysis

For graph theory evaluation, statistical analysis was conducted using a general linear model (GLM), with each graph-theoretical network metric (GE, LE, CC, SW, NE, ND, BC) serving as a dependent variable. The model included READ1d, mean reading performance, and their interaction as primary predictors, while sex, age, IQ, and DSM inattention scores were included as covariates to

account for potential confounds (see the 'Neuropsychological Assessment' paragraph).

To assess potential multicollinearity, Spearman correlation matrices were computed for all covariates included in the GLM (age, sex, IQ, and DSM inattention scores), both for the full sample and stratified by diagnostic group (Supplementary Materials, Fig. S2). Variance inflation factors (VIFs) were additionally computed showing a low and not concerning collinearity among covariates (Supplementary Materials, Table S2).

To correct for multiple comparisons across the 82 nodes of the connectome, we applied the Statistical Parametric Connectome (SPC) framework (Meskaldji et al. 2015). SPC is specifically designed for connectome-level inference, offering increased sensitivity and specificity by exploiting known dependencies within brain networks. Indeed, compared to standard FDR or Bonferroni correction methods, SPC has demonstrated superior performance in both simulation studies and real neuroimaging datasets (Meskaldji et al. 2015; Fischi-Gómez et al. 2015). It employs an adaptive strategy that leverages either the statistical structure of the connectome or prior knowledge about topological dependencies (e.g., positive correlations between connected nodes). The method first decomposes the connectome into subnetworks, which can be defined either a priori or via clustering algorithms.

In this study, subnetworks were defined using two complementary approaches:

1. Anatomical grouping, where nodes were assigned to cortical lobes;
2. Walktrap community detection, a data-driven algorithm that identifies modular structures based on network topology. The clustering was applied on the group-average structural connectome, obtained by averaging the matrices across all $N = 74$ participants prior to graph construction.

In the following, we will report just the results from method 2, with method 1 showing a high level of overlapping (see Supplementary Materials, Table S3).

For each nodal metric (nodal degree, nodal local efficiency, betweenness centrality), the full GLM was fitted at each node. The model p-values were entered into the SPC procedure, with significance declared at FDR-corrected $p \leq .05$.

For nodes passing this threshold, we subsequently extracted and reported the predictor-specific p-values and unstandardised regression coefficients (β) associated with each primary predictor of interest (READ1d, mean reading, and their interaction), as derived from the GLM. These predictor-level statistics are reported to characterise the direction and magnitude of individual predictor contributions within the set of nodes already identified as significant at the model level and should be interpreted as exploratory.

A schematic overview of the entire processing and analysis pipeline is presented in Fig. 1.

All statistical analyses were performed in RStudio (v2022.02.1). Network visualizations were generated in Python using the *nibabel* library, with node coordinates extracted from the atlas via the FreeSurfer function *mri2surfer*.

Sensitivity analyses were conducted using the G*Power software, Version 3.1.9.2 (Faul et al. 2007, 2009), to compute the smallest effect size that our samples could detect with at least 80% statistical power. As a model, we selected

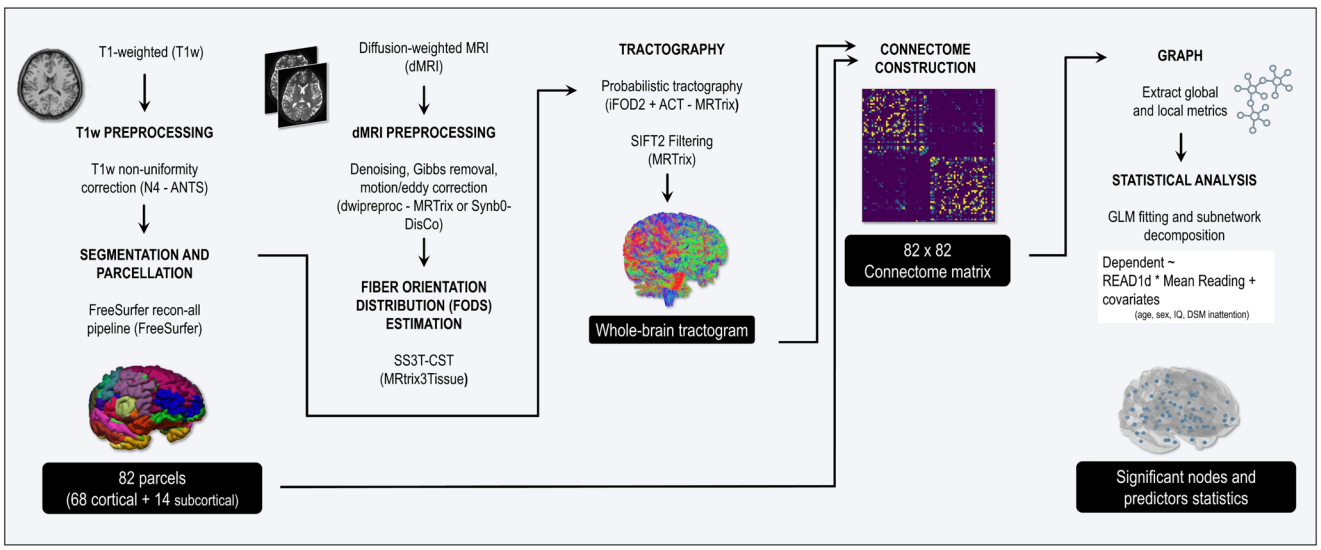

Fig. 1 Flow diagram summarizing the methodological workflow, including imaging preprocessing, tractography, connectome construction, and graph-theoretical analysis

Table 1 Descriptive statistics

Variable	Whole group $N=74$	DDnd $n=19$	DDd $n=17$	TRnd $n=22$	TRd $n=16$	Statistic	p	ES	Post-hoc
Gender (male/female)	47/27	13/4	14/5	6/10	14/8	$\chi^2(3)=6.75$	0.080	0.30	
Age [months]	161 (22)	173 (23)	169 (21)	156 (19)	146 (17)	$H(3)=14.85$	0.002**	0.20	DDnd > TRd (p=.018) DDd > TRd (p=.004)
Mean reading	-1.35 (2.09)	-2.82 (1.66)	-3.26 (1.88)	0.23 (0.36)	0.32 (0.31)	$H(3)=55.30$	<0.001***	0.76	DDnd < TRnd (p<.001) DDd < TRnd (p<.001) DDnd < TRd (p<.001) DDd < TRd (p<.001)
DSM inattention	53 (11)	59 (13)	58 (12)	47 (7)	50 (7)	$H(3)=13.93$	0.003**	0.19	DDnd > TRnd (p=.014) DDd > TRnd (p=.014)
IQ°	13 (3)	12 (3)	11 (2)	14 (4)	12 (2)	$F(3,70)=5.23$	0.003**	0.18	TRnd > DDnd (p=.002) TRnd > TRd (p=.025)
Socioeconomic status	59.86 (18.56)	64.71 (20.95)	51.18 (14.53)	59.38 (18.34)	63.18 (18.36)	$H(3)=4.34$	0.227	0.08	

Mean (SD) reported for continuous variables. The p-value column refers to $\chi 2$ test for gender, ANOVA for IQ, and Kruskal-Wallis for the other variables, due to not normality. The ES (Effect Size) column refers to ε^2 (Kruskal-Wallis), η^2 (ANOVA), V (chi-square). The Post-hoc column refers to Dunn test with Bonferroni correction (Kruskal-Wallis); Tukey HSD (ANOVA)

Level of significance $p<.05$ (*), $p<.01$ (**), $p<.001$ (***)

°As estimated by the vocabulary and block design subscales of the WISC-III (Wechsler 2006).

Table 2 Global metrics results

	Predictor	β mean	β std	95% CI	p-value	β stand	η^2	Cohen's d	adj-R^2
GE	READ1d	−6.68e−3	2.79e−3	[−1.22e−2; −1.11e−3]	0.019*	−0.555	0.080	−0.624	0.210
	Mean reading	7.54e−4	7.97e−4	[−8.37e−4; 2.35e−3]	0.347	0.150	0.013	–	0.210
	READ1d × mean reading	−6.13e−4	1.13e−3	[−2.88e−3; 1.65e−3]	0.591	−0.122	0.004	–	0.210
SW	READ1d	−1.85e−1	4.02e−1	[−9.88e−1; 6.17e−1]	0.646	−0.159	0.003	−0.161	0.025
	Mean reading	5.04e−2	1.15e−1	[−1.79e−1; 2.80e−1]	0.662	0.077	0.003	–	0.025
	READ1d × mean reading	2.37e−2	1.64e−1	[−3.03e−1; 3.50e−1]	0.885	0.036	<0.001	–	0.025
LE	READ1d	−6.61e−4	2.89e−4	[−1.24e−3; −8.36e−5]	0.025*	−0.528	0.073	−0.581	0.174
	Mean reading	4.77e−5	8.27e−5	[−1.17e−4; 2.13e−4]	0.566	0.094	0.005	–	0.174
	READ1d × mean reading	−7.15e−5	1.18e−4	[−3.07e−4; 1.64e−4]	0.546	−0.141	0.006	–	0.174
CC	READ1d	−8.50e−4	3.65e−4	[−1.58e−3; −1.22e−4]	0.023*	−0.562	0.076	−0.618	0.175
	Mean reading	3.27e−5	1.04e−4	[−1.75e−4; 2.41e−4]	0.755	0.051	0.002	–	0.175
	READ1d × mean reading	−6.79e−5	1.48e−4	[−3.64e−4; 2.28e−4]	0.649	−0.106	0.003	–	0.175

GE global efficiency; *SW* small worldness; *CC* clustering coefficient; *LE* local efficiency

Level of significance $p<.05$ (*)

"ANCOVA with fixed effects, main effects and interactions"; α was set at the Bonferroni-corrected level (0.0125), $n=74$, power = 0.80. Under these assumptions, the minimal detectable effect size was 0.434.

Results

Sample

The final cohort comprised 74 subjects, grouped in 17 subjects with DD and READ1d (DDd), 19 subjects with DD without READ1d (DDnd), 16 TRs with READ1d (TRd), and 22 TRs without READ1d (TRnd). Descriptive statistics for demographic and neuropsychological measures and socioeconomic status for the four groups are reported in Table 1. Age, mean reading, DSM inattention and IQ are all significantly different among the groups, justifying their inclusion as covariates in further analyses (see 'Statistical analysis' paragraph). Contrary, the groups do not differ for socioeconomic status, that was indeed not included as covariate. Spearman correlation between READ1d and Mean Reading score was non-significant ($\rho=.020$, $p=.863$).

Global metrics

Table 2 reports the results of statistical analysis for the global metrics. READ1d carrier status was associated with nominally ($p<.05$, not-corrected) lower GE, LE and CC, with READ1d carriers showing consistently lower values than non-carriers across all three metrics. Effect sizes were in the medium range across all three outcomes. SW did not differ between groups. No effects of mean reading and

READ1d * Mean reading interactions were found on any global metrics.

Local metrics

Figure 2 shows the clusters resulting from the Walktrap algorithm applied on the average connectome. Except for Cluster 3 which extends across both hemispheres in a symmetrical way, all the other identified clusters encompass regions from different lobes but remain confined within a single hemisphere.

At the nodal level, different brain nodes ($n=25$) were significantly associated with both mean reading and READ1d (Fig. 3). In particular, consistent negative associations between READ1d and ND emerged across several cortical areas ($n=17$) (Fig. 3, upper panel). Specifically, subjects with READ1d showed lower ND in bilateral temporal (L-IT, L-ST, L-TT, R-Bnk, R-ST, R-TT), bilateral occipital (L-Cun, L-Pcal, R-LO, R-Pcal, R-Cun), bilateral frontal (L-PTri, L-RMF, R-CMF, R-PTri, R-RMF) nodes, and in a parietal supra-marginal left node (L-SM). Except for an outlier which showed negative association (L-Ent), better reading proficiency was associated with increased ND in several nodes ($n=13$), particularly in the left parieto-occipital lobe (L-Cun, L-IP, L-LO, L-PCe, L-Pcal, L-PreC, L-SP, L-SM) and in the right hemisphere (R-Cun, R-PCe, R-SP, R-TT, R-CMF) (Fig. 3, lower panel). No significant READ1d*Mean Read effect was found on ND.

While ND exhibits a relatively consistent pattern across nodes, NE displays greater variability. Significant effects of READ1d and Mean Reading were observed on NE within 18 nodes (Fig. 4). In particular, individuals with READ1d showed lower mean values in 14 nodes within the bilateral frontal (L-RMF, R-RMF), bilateral temporo-parietal (L-ST, R-ST, R-Bnk, R-PCe, R-SM, R-TT) and the right occipital (Pcal, Cun) regions, as well as within left amygdala, right accumbens and bilateral insula (Fig. 4, upper panel). Better reading proficiency was associated with lower NE in bilateral temporo-parietal regions (L-IT, L-ST, R-MT, R-SM) and the right accumbens, but with higher NE in the left occipital cortex (L-Cun, L-PCal) and right paracentral cortex (Fig. 4, lower panel). As for ND, no significant READ1d*Mean reading interaction effects were found on NE (Fig. 4).

No statistically significant effects of READ1d, Mean reading and READ1d*Mean reading interaction were found on BC.

Discussion

The structural and genetic underpinnings of DD have been widely studied, but the heterogeneity of the disorder and the complexity of the reading network have led to findings that are often only partially consistent (Moreau et al. 2018). Furthermore, even if research about genes and structural

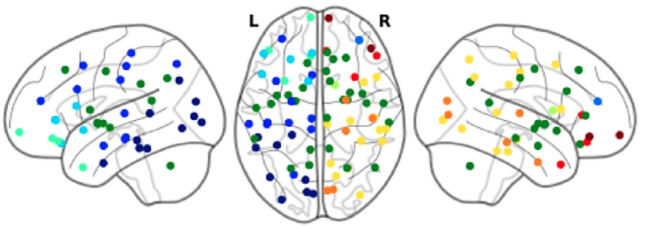

Original Label	Abbreviation
ctx-bankssts	Bnk
ctx-caudalanteriorcingulate	CAC
ctx-caudalmiddlefrontal	CMF
ctx-cuneus	Cun
ctx-entorhinal	Ent
ctx-fusiform	Fus
ctx-inferiorparietal	IP
ctx-inferiortemporal	IT
ctx-isthmuscingulate	Isth
ctx-lateraloccipital	LO
ctx-lateralorbitofrontal	LOrF
ctx-lingual	Lin
ctx-medialorbitofrontal	MOrF
ctx-middletemporal	MT
ctx-parahippocampal	PH
ctx-paracentral	PCe
ctx-parsopercularis	POp
ctx-parsorbitalis	POrb
ctx-parstriangularis	PTri
ctx-pericalcarine	Pcal
ctx-postcentral	PostC
ctx-posteriorcingulate	PCi
ctx-precentral	PreC
ctx-precuneus	PCun
ctx-rostralanteriorcingulate	RAC
ctx-rostralmiddlefrontal	RMF
ctx-superiorfrontal	SF
ctx-superiorparietal	SP
ctx-superiortemporal	ST
ctx-supramarginal	SM
ctx-frontalpole	FP
ctx-temporalpole	TP
ctx-transversetemporal	TT
ctx-insula	Ins
cerebellum-cortex	CbC
caudate	Cd
putamen	Put
pallidum	Pal
hippocampus	Hpc
amygdala	Amy
accumbens-area	Acc

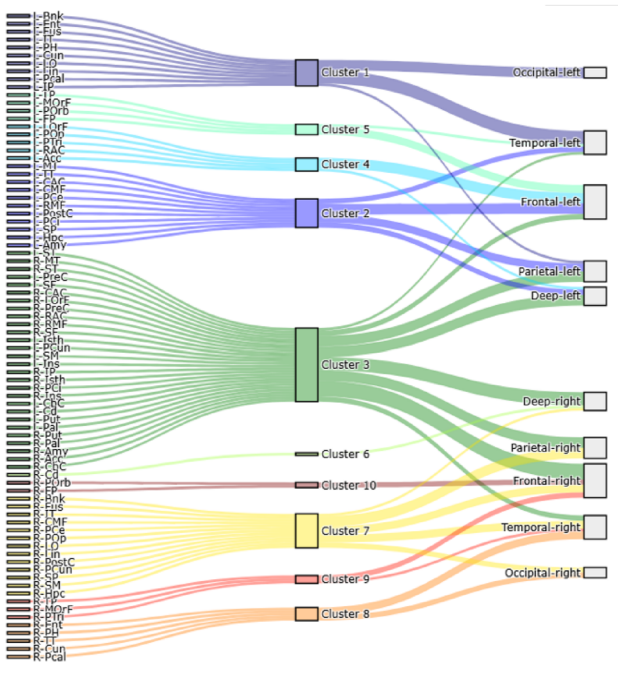

Fig. 2 Node clustering from the Walktrap algorithm, accompanied by a table of their abbreviations. Nodes are bilateral; therefore, each is referred to by its hemisphere (left [L] or right [R]) followed by the corresponding abbreviation. On the right, a Sankey diagram illustrates the assignment of each node to both its Walktrap cluster and its corresponding lobe

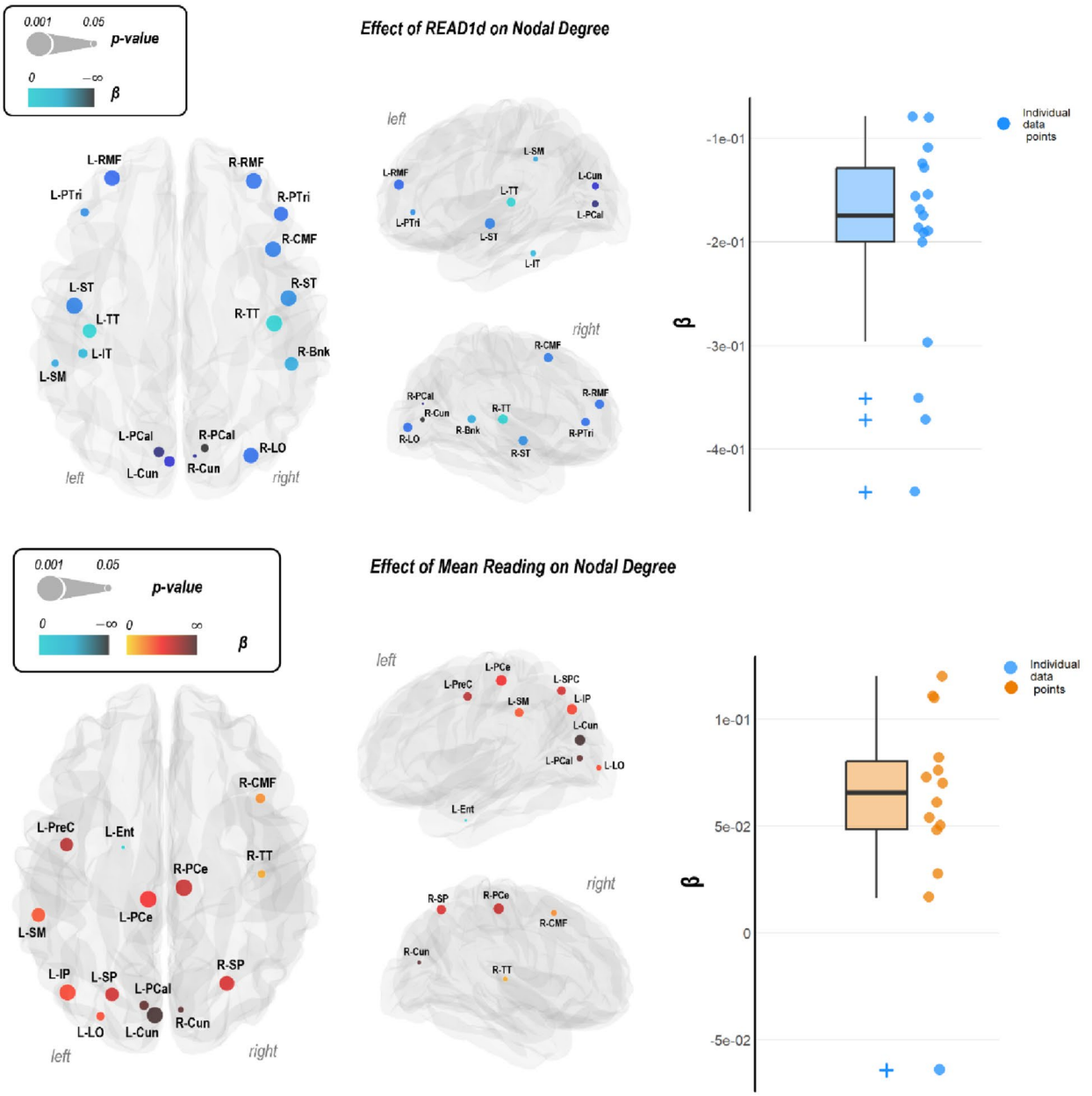

Fig. 3 Effect of READ1d and mean reading on nodal degree (ND). The figure displays nodes showing significant associations after SPC-based FDR correction. Marker size is proportional to statistical significance, such that larger markers indicate more significant associations (p-values derived from Type II ANOVA on the primary GLM). Colour intensity is proportional to the regression coefficients (β), with darker shading indicating larger effect sizes; the accompanying boxplot illustrates the distribution of β coefficients across significant nodes. For additional details on node labels and anatomical regions, see Supplementary Materials, Figs. S3 and S4

alteration (considered separately) are numerous (for a complete review, see Mascheretti et al. 2017; Landi and Perdue 2019), relatively few works have considered the two factors at the same time, mainly by focusing on WM integrity or DTI derived parameters (Darki et al. 2014; Marino et al. 2012, 2014; Perani et al. 2021). Here, we integrated genetic information with connectome metrics in order to provide network-level evidence that genetic liability may relate to WM network organization and properties in brain areas underlying reading proficiency. This led us to provide systematic evidence to previous speculations suggesting brain organization may have a genetic origin linked to DD candidate genes (Lou et al. 2019). We therefore investigated

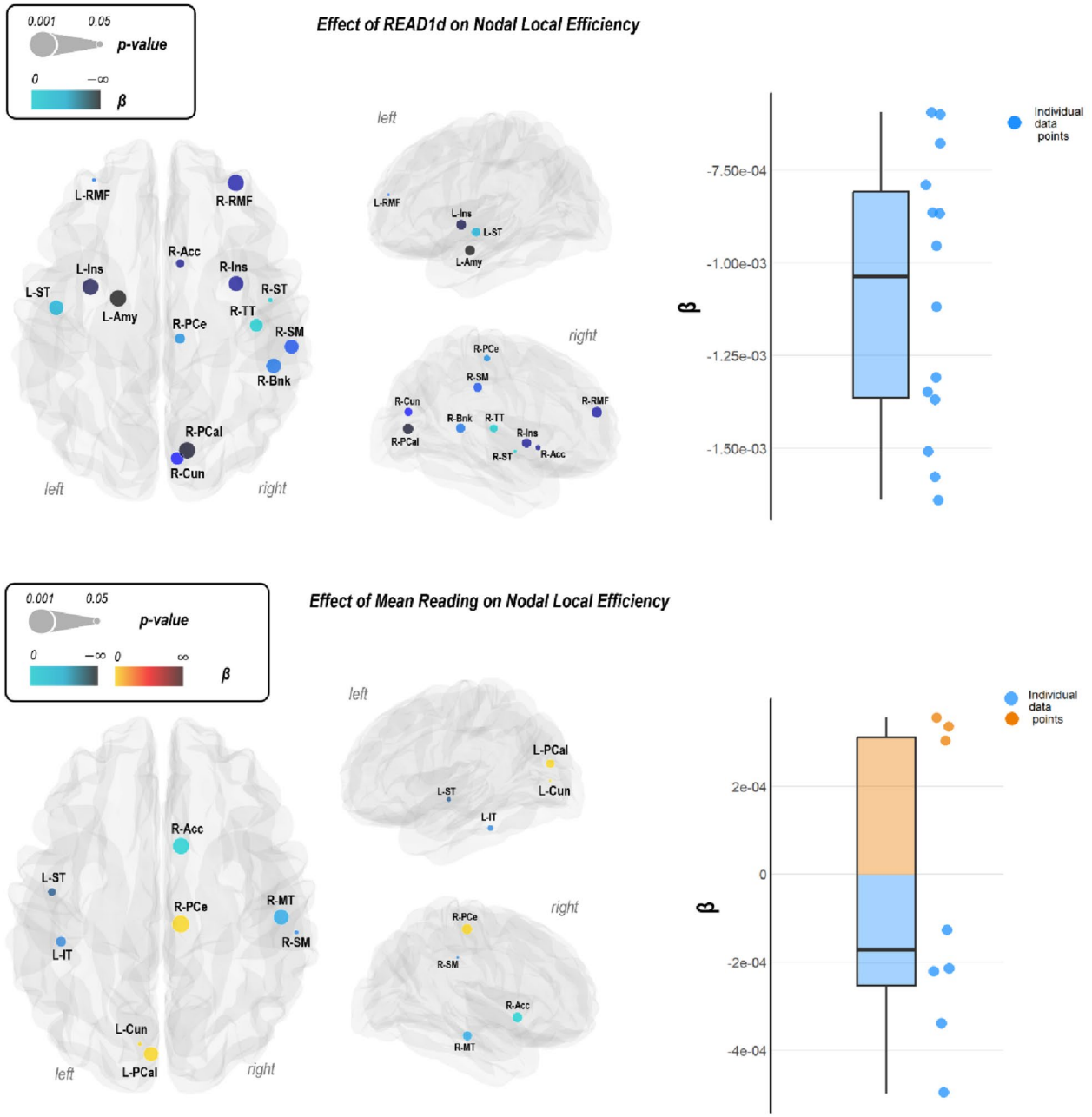

Fig. 4 Effect of READ1d and mean reading on nodal local efficiency (NE). The figure displays nodes showing significant associations after SPC-based FDR correction. Marker size is proportional to statistical significance, such that larger markers indicate more significant associations (p-values derived from Type II ANOVA on the primary GLM). Colour intensity is proportional to the regression coefficients (β), with darker shading indicating larger effect sizes; the accompanying boxplot illustrates the distribution of β coefficients across significant nodes. For additional details on node labels and anatomical regions, see Supplementary Materials, Figs. S5 and S6

differences in connectomes linked to the READ1d-moderated genetic vulnerability and reading proficiency.

From a methodological viewpoint, we moved from the local voxel-wise analysis to graph-theoretical analysis encompassing the global brain architecture to investigate the scenario with grained detail. Furthermore, we applied a more advanced model (CSD) to overcome the inherent limitations of more conventional DTI approaches (Farquharson et al. 2013). Despite the lack of higher b-values shells (generally required for this kind of models), we try to follow the usual guidelines to avoid the most common pitfalls (Jones and Cercignani 2010; Calamante 2019) in

connectivity analysis. More broadly, even applying best practices (Tahedl et al. 2025), we are aware that connectome construction involves numerous sequential processing decisions, from tractography algorithm and seeding strategy to streamline filtering and edge weight definition. Each of these choices can influence the resulting graph metrics. Indeed, it is important to note that the present findings should be interpreted in the context of the specific pipeline employed. As a sensitivity analysis, results were replicated using SIFT rather than SIFT2 tractography filtering. While both methods address the same tractography bias, they differ in whether connectivity is estimated from a filtered subset of streamlines (SIFT) (Smith et al. 2012) or from the full tractogram with per-streamline weights (SIFT2) (Smith et al. 2015). Consistency across both approaches indicates that the findings are not specific to the weighting scheme (Supplementary Materials, Table S4), though replication using alternative parcellations or edge weight definitions would provide a more comprehensive assessment of pipeline robustness.

Furthermore, in connectome related studies, potential limits arise not only from the connectome construction, but also from statistical modeling and significant threshold assessment. To address this, we applied a multiple-testing correction method specifically tailored for connectomes, which preserves network topology and considers the brain as an integrated system rather than a collection of independent nodes. This choice was particularly crucial given that the expected structural differences between typical and dyslexic readers are subtle, as revealed by meta analysis studies (Moreau et al. 2018; Ramus et al. 2018). To address this aspect, we adopted a connectome-level inferential framework tailored to network structure (SPC) (Meskaldji et al. 2015). The node clustering analysis serves a statistical rather than descriptive purpose. When testing effects across 82 nodes simultaneously, standard multiple comparisons corrections (Bonferroni, FDR) treat each node as independent. But this assumption is violated in connectome data, since spatially proximal and functionally related nodes show correlated effects (Meskaldji et al. 2015). The Walktrap community detection algorithm identifies data-driven subnetworks of correlated nodes. By grouping nodes into communities and correcting within the entire connectome, SPC exploits the known dependency structure of brain networks to increase sensitivity while controlling the false discovery rate. This means that the community structure itself is a statistical substrate that enables valid inference at the nodal level.

Overall, our results revealed slight but significant differences related to both READ1d and reading proficiency. In particular, READ1d carrier status was associated with nominally significant lower global efficiency, local efficiency, and clustering coefficient compared to non-carriers, with consistent effect directions across all three metrics. Taken together, these findings point to a specific effect of READ1d on network integration and segregation. Moreover, at the nodal level, we found that subjects with READ1d exhibited reduced nodal degree and local nodal efficiency in bilateral temporal, parietal and frontal regions. Although different methodological techniques were applied, previous studies investigating the relationship between *DCDC2* and WM integrity have emphasized local left-hemispheric alterations particularly in the arcuate fasciculus and temporo-parietal regions (Darki et al. 2014; Marino et al. 2012), suggesting that the global integration/segregation deficit may be the result of local alteration of the fiber structure. Our results revealed bilateral effects suggesting that the overall impact of READ1d is not strictly confined to left-lateralized language tracts, but extends to a broader bilateral network (Darki et al. 2014). Furthermore, the nodes influenced by READ1d align with regions which are affected by different level of DCDC2 expression, i.e., hippocampus, entorhinal cortex, hypothalamus, amygdala, inferior and medial temporal cortex (Meng et al. 2005; Paracchini et al. 2007; Meda et al. 2008). Taken together these results are consistent with the effects of READ1d on the dorsal stream networks which is crucial in reading development. Among the numerous theories trying to elucidate the mechanism behind DD, a prominent line converges on a magnocellular deficit hypothesis which posits that impaired processing in the dorsal visual stream may contribute to reading difficulties (Stein and Walsh 1997; Livingstone et al. 1991). This theory hypothesizes that DD is due to a multimodal sensory impairment in the processing of transient and dynamic stimuli (Stein and Talcott 1999; Gori et al. 2016) which arises from a deficit along the neural pathways involved in the fast transmission and processing of sensory information (Stein 2001, 2014). By providing additional data about the role of READ1d within the structural and functional properties of the dorsal stream Mascheretti et al. 2021, 2024; Cicchini et al. 2015; Marino et al. 2012; Perani et al. 2021), our results are in line with a more widespread integration deficit among the different areas involved in a specific portion of the reading circuit.

Regarding the reading proficiency, we found significant correlations with both nodal degree and nodal local efficiency in nodes that can be linked to tracts within the reading circuit (for a complete overview see Vandermosten et al. 2012). Indeed, superior-temporal nodes (e.g., L-IT, L-ST, R-ST, L-PTri, L-RMF, R-MT, R-SM) are commonly connected *via* the arcuate and superior longitudinal fasciculi, while occipital nodes (e.g., L-Cun, L-Pcal) are associated with the inferior longitudinal fasciculus, and the supramarginal node (L-SMG) represent the end point of the arcuate

fasciculus. However, reading skills showed mixed correlations with nodal degree (mostly positive) and nodal local efficiency (mostly negative). Although these results may appear contradictory, they are consistent with the understanding that local efficiency, unlike global efficiency, is highly sensitive to node-specific variations and local network characteristics (Jiang et al. 2023). Importantly, these patterns likely reflect distinct mechanisms. Specifically, the inverse association between nodal local efficiency and mean reading may indicate that, although the brain network generally balances integration and segregation, a decrease in the nodal local efficiency can correspond to greater functional specialization. Supporting this view, previous studies have shown that lower nodal local efficiency can be associated with higher cognitive performance (Stanley et al. 2015) or can manifest differently across individual nodes depending on their functional role (Xu et al. 2015).

A key result of our study is the absence of a significant interaction between READ1d and reading ability at the structural level. This contrasts with prior reports of significant genotype and reading interactions in both WM integrity and functional activation in comparable cohorts (Marino et al. 2014; Mascheretti et al. 2024). Discrepancies with Marino and colleagues (2014) likely reflect both population and methodological factors. Regarding the sample, their cohort was older than ours, so the observed interaction may capture an age-related consolidation of DD-related brain differences. In other words, it is not possible to exclude that the structural variations may reflect less exposure to reading rather than a primary cause of DD (Krafnick et al. 2014). In contrast, our sample consisted of relatively younger readers (mean age 13 years), a condition that allows us to observe neurobiological correlates at an early stage of development, reducing the influence of secondary factors related to reading experience. Moreover, whereas Marino et al. (2014) focused on tract-specific microstructural alterations within major fasciculi, our analyses target whole-brain network interactions among cortical regions. Concerning the discrepancy with functional analyses previously conducted on a similar cohort (Mascheretti et al. 2024), we argue that it may reflect the complementary nature of structural and functional measures. The relation between structural and functional connectivity is not linear (Litwińczuk et al. 2022) and the existence of functional relationships between couples of regions does not necessarily imply the presence of a direct structural connection between them (Honey et al. 2009). The absence of a significant READ1d × Mean Reading interaction across both global and nodal metrics suggests that the association between READ1d carrier status and WM network organisation does not vary as a function of reading proficiency. This is consistent with the possibility that READ1d is associated with broad differences in network organisation that are not coupled to reading proficiency within the range examined here. To confirm that this null interaction does not affect the primary findings, results from a reduced additive model excluding the interaction term are reported in Supplementary Materials, Table S5; these were fully consistent with the primary analysis in both direction and significance.

Taken together, READ1d-related anatomical patterns, irrespective of reading proficiency, may mark some subthreshold developmental vulnerability to cognitive deficits. This is compatible with the hypothesis that some risk variants of genes implicated in neuronal migration influence brain development, and lead to neuroanatomical variations underlying DD (Galaburda et al. 2006). Likewise, these findings agree with the multifactorial threshold model of the liability to reading disability (Pennington 2006; McGrath et al. 2011). Reading skills represent the final outcome of multiple genetic and environmental components that vary widely across individuals, the READ1d-related anatomical patterns may contribute to DD and/or other cognitive phenotypes depending on co-occurring risk factors. In other words, the observation that READ1d carriers show differences in WM network organisation regardless of diagnostic status is consistent with the multifactorial threshold model of reading disability (McGrath et al. 2011), in which reading outcome reflects the cumulative effect of multiple genetic and environmental factors, and a single variant does not determine the phenotype. Under this framework, READ1d is one of several factors associated with reading risk. The TR carriers in the present sample are particularly informative in this regard: individuals who carry the deletion but read within the typical range nonetheless show network profiles more similar to DD carriers than to non-carriers. Whether this pattern constitutes a latent vulnerability marker that precedes the clinical expression of reading difficulties warrants investigation in future longitudinal studies.

This study has several limitations that should be acknowledged. First, the sample size ($N = 74$) is relatively small and may have reduced statistical power, increasing the likelihood of false-negative. Even if our sample is comparable to those used in prior imaging–genetics studies (Darki et al. 2012, 2014; Marino et al. 2012; Perani et al. 2021; Mascheretti et al. 2024), sensitivity analyses indicated that the minimum detectable effect size at 80% power with Bonferroni correction was $f = 0.434$, suggesting that small-to-medium effects may have been missed. Future studies with larger, prospectively recruited cohorts are needed to confirm and extend the present findings. Second, the four subgroups differed significantly in age, sex, IQ, and inattention scores. To mitigate potential confounding effects, all of these variables were included as covariates in the statistical analyses. To further address this discrepancy, we performed propensity

score matching on age, sex, DSMinattention and IQ; results overlapped with those obtained with the original sample (see Supplementary Materials, Table S6) supporting the robustness of the main findings. Furthermore, the dMRI dataset was acquired at the lower limit of what is optimal for the application of advanced modeling techniques such as those employed here. However, SS3T-CSD has previously been shown to yield reliable results even with less optimal acquisition schemes (Dhollander et al. 2019; Rauland et al. 2025), reaching a good compromise with the constraints of clinical applications. In addition, we constructed connectomes weighted by volume. While this is a common choice, alternative weighting strategies (e.g., FA) might capture complementary aspects of WM organization and could be explored in future works. Despite these limitations, and although the present findings should be considered preliminary and exploratory given the modest sample size and the nominal significance of the global metric associations, they underscore the translational potential of connectomics as a framework for linking genetic variation to large-scale brain network organisation.

Conclusion

This study investigated the relationship between a genetic variant commonly associated with DD, reading proficiency and measures of connectivity and structural integrity of WM fibers in the central nervous system. Our findings suggest that READ1d is likely associated with reduced efficiency and segregation of structural connectivity mainly within the visual dorsal. This alteration in structural connectivity may represent a vulnerability factor for DD which may help to optimize the diagnostic criteria and thereby facilitate the early identification of children with genetically-driven susceptibility.

Supplementary Information The online version contains supplementary material available at https://doi.org/10.1007/s00429-026-03160-2.

Acknowledgements The authors gratefully acknowledge Dr. Nicola Pesenti for his support with the statistical analyses.

Author contributions M. Di Stefano: Writing – review & editing, Writing – original draft, Visualization, Conceptualization, Software, Formal analysis. S. Mascheretti: Writing – review & editing, Writing – original draft, Conceptualization, Resources. V. Lampis: Writing – review & editing, Conceptualization, Resources. F. Maccarone: Software, Writing – review & editing. C. Mauri: Writing – review & editing. M. Di Segni: Writing – review & editing. D. Peruzzo: Writing – review & editing, Supervision, Conceptualization.

Funding The authors have not disclosed any funding. This study was supported by Italian Ministry of Health (Ricerca Corrente "2024-26" to Denis Peruzzo, Valentina Lampis, and Chiara Mauri).

Data availability The datasets used and/or analysed during the current study will be available from the corresponding author on reasonable request.

Declarations

Conflict of interest The authors declare no competing interests.

References

American Psychiatric Association (2006) Diagnostic and Statistical Manual of Mental Disorders, 4th edn. American Psychiatric Association, Washington, DC

Andreola C, Mascheretti S, Belotti R et al (2021) The heritability of reading and reading-related neurocognitive components: A multilevel meta-analysis. Neurosci Biobehav Rev 121:175–200. https://doi.org/10.1016/j.neubiorev.2020.11.016

Arina S, Iervolino I, Stella G (2013) Prima raccolta di dati normativi per la valutazione della dislessia evolutiva negli adolescenti su un campione di scuola secondaria di secondo grado. Dislessia 10:9–38

Basser PJ, Mattiello J, LeBihan D (1994) MR diffusion tensor spectroscopy and imaging. Biophys J 66(1):259–267. https://doi.org/10.1016/S0006-3495(94)80775-1 PMID:8130344; PMCID:PMC1275686

Beaulieu C, Plewes C, Paulson LA, Roy D, Snook L, Concha L, Phillips L (2005) Imaging brain connectivity in children with diverse reading ability. NeuroImage 25:1266–1271

Behrens TE, Berg HJ, Jbabdi S, Rushworth MF, Woolrich MW (2007) Probabilistic diffusion tractography with multiple fibre orientations: What can we gain? NeuroImage 34(1):144–155. https://doi.org/10.1016/j.neuroimage.2006.09.018

Boets B, Op de Beeck HP, Vandermosten M et al (2013) Intact but less accessible phonetic representations in adults with dyslexia. Science 342:1251–1254

Brkanac Z, Chapman NH, Matsushita MM, Chun L, Nielsen K, Cochrane E, Berninger VW, Wijsman EM, Raskind WH (2007) Evaluation of candidate genes for DYX1 and DYX2 in families with dyslexia. Am J Med Genet B Neuropsychiatr Genet 144B(4):556–560. https://doi.org/10.1002/ajmg.b.30471

Calamante F (2019) The seven deadly sins of measuring brain structural connectivity using diffusion MRI streamlines fibre-tracking. Diagnostics 9:115. https://doi.org/10.3390/diagnostics9030115

Carrion-Castillo A, Franke B, Fisher SE (2013) Molecular genetics of dyslexia: An overview. Dyslexia 19(4):214–240. https://doi.org/10.1002/dys.1464PMID:24133036

Cicchini GM, Marino C, Mascheretti S, Perani D, Morrone MC (2015) Strong motion deficits in dyslexia associated with DCDC2 gene alteration. J Neurosci 35(21):8059–8064. https://doi.org/10.1523/JNEUROSCI.5077-14.2015

Conners CK (1989) Manual for Conners' Rating Scales. Multi-Health Systems, North Tonawanda, NY

Conners CK, Sitarenios G, Parker JDA, Epstein JN (1998) The Revised Conners' Parent Rating Scale (CPRS-R): Factor structure, reliability, and criterion validity. J Abnorm Child Psychol 26(4):257–268. https://doi.org/10.1023/A:1022658222914

Cope N, Eicher JD, Meng H, Gibson CJ, Hager K, Lacadie C et al (2012) Variants in the DYX2 locus are associated with altered brain activation in reading-related brain regions in subjects with reading disability. NeuroImage 63(1):148–156

Cornoldi C (1995) Nuove Prove di Lettura MT per la Scuola Media Inferiore. Organizzazioni Speciali, Firenze, Italy

Cornoldi C, Carretti B (2016) Prove MT Avanzate-3-Clinica: La Valutazione delle Abilità di Lettura, Comprensione, Scrittura e Matematica per il Biennio della Scuola Secondaria di II Grado; Giunti Edu: Florence, Italy

Cornoldi C, Colpo G (1998) Prove di Lettura MT per la Scuola Elementare, 2nd edn. Organizzazioni Speciali, Firenze, Italy

Darki F, Peyrard-Janvid M, Matsson H, Kere J, Klingberg T (2012) Three dyslexia susceptibility genes, DYX1C1, DCDC2, and KIAA0319, affect temporo-parietal white matter structure. Biol Psychiatry 72(8):671–676. https://doi.org/10.1016/j.biopsych.2012.05.008

Darki F, Peyrard-Janvid M, Matsson H, Kere J, Klingberg T (2014) DCDC2 polymorphism is associated with left temporoparietal gray and white matter structures during development. J Neurosci 34:14455–14462

Desikan RS, Ségonne F, Fischl B, Quinn BT, Dickerson BC, Blacker D, Buckner RL, Dale AM, Maguire RP, Hyman BT, Albert MS, Killiany RJ (2006) An automated labeling system for subdividing the human cerebral cortex on MRI scans into gyral-based regions of interest. NeuroImage 31(3):968–980. https://doi.org/10.1016/j.neuroimage.2006.01.021

Deutsch GK, Dougherty RF, Bammer R, Siok WT, Gabrieli JDE, Wandell B (2005) Children's reading performance is correlated with white matter structure measured by diffusion tensor imaging. Cortex 41:354–363

Dhollander T, Connelly A (2016) A novel iterative approach to reap the benefits of multi-tissue CSD from just single-shell (+b=0) diffusion MRI data. Proc Int Soc Magn Reson Med

Dhollander T, Mito R, Raffelt D, Connelly A (2019) Improved white matter response function estimation for 3-tissue constrained spherical deconvolution. Proc Int Soc Magn Reson Med

Farahani FV, Karwowski W, Lighthall NR (2019) Application of Graph Theory for Identifying Connectivity Patterns in Human Brain Networks: A Systematic Review. Front Neurosci 13:585. https://doi.org/10.3389/fnins.2019.00585

Farquharson S, Tournier J, Calamante F, Fabinyi G, Schneider-Kolsky M, Jackson GD, Connelly A (2013) White matter fiber tractography: Why we need to move beyond DTI. J Neurosurg 118(6):1367–1377. https://doi.org/10.3171/2013.2.JNS121294

Faul F, Erdfelder E, Lang A-G, Buchner A (2007) G*Power 3: a flexible statistical power analysis program for the social, behavioral, and biomedical sciences. Behav Res Methods 39:175–191. https://doi.org/10.3758/BF03193146

Faul F, Erdfelder E, Buchner A, Lang AG (2009) Statistical power analyses using G*Power 3.1: tests for correlation and regression analyses. Behav Res Methods 41(4):1149-60. https://doi.org/10.3758/BRM.41.4.1149

Fischi-Gómez E, Vasung L, Meskaldji DE, Lazeyras F, Borradori-Tolsa C, Hagmann P, Barisnikov K, Thiran JP, Hüppi PS (2015) Structural brain connectivity in school-age preterm infants provides evidence for impaired networks relevant for higher order cognitive skills and social cognition. Cereb Cortex 25(9):2793–2805. https://doi.org/10.1093/cercor/bhu073

Galaburda AM (1993) Neurology of developmental dyslexia. Curr Opin Neurobiol 3(2):237–242. https://doi.org/10.1016/0959-4388(93)90216-l

Galaburda AM, LoTurco J, Ramus F, Fitch RH, Rosen GD. From genes to behavior in developmental dyslexia. Nat Neurosci. 2006 Oct;9(10):1213-7. https://doi.org/10.1038/nn1772

Gori S, Seitz AR, Ronconi L, Franceschini S, Facoetti A (2016) Multiple causal links between magnocellular–dorsal pathway deficit and developmental dyslexia. Cereb Cortex 26(11):4356–4369

Greven CU, Harlaar N, Dale PS, Plomin R (2011) Genetic Overlap between ADHD Symptoms and Reading is largely Driven by Inattentiveness rather than Hyperactivity-Impulsivity. J Can Acad Child Adolesc Psychiatry 20(1):6–14

Greven CU, Rijsdijk FV, Asherson P, Plomin R (2012) A longitudinal twin study on the association between ADHD symptoms and reading. J Child Psychol Psychiatry 53(3):234–242. https://doi.org/10.1111/j.1469-7610.2011.02445.x

Harold D, Paracchini S, Scerri T, Dennis M, Cope N, Hill G, Moskvina V, Walter J, Richardson AJ, Owen MJ, Stein JF, Green ED, O'Donovan MC, Williams J, Monaco AP (2006) Further evidence that the KIAA0319 gene confers susceptibility to developmental dyslexia. Mol Psychiatry 11(12):1085–1091. https://doi.org/10.1038/sj.mp.4001904

Hollingshead AB (1975) Four factor index of social status. Yale University, New Haven, CT

Honey CJ, Sporns O, Cammoun L, Gigandet X, Thiran JP, Meuli R, Hagmann P (2009) Predicting human resting-state functional connectivity from structural connectivity. Proc Natl Acad Sci USA 106(6):2035–2040. https://doi.org/10.1073/pnas.0811168106

Jelescu IO, Budde MD (2017) Design and validation of diffusion MRI models of white matter. Front Phys 28:61. https://doi.org/10.3389/fphy.2017.00061

Jiang W, Zhou Z, Li G, Yin W, Wu Z, Wang L, Ghanbari M, Li G, Yap PT, Howell BR, Styner MA, Yacoub E, Hazlett H, Gilmore JH, Keith Smith J, Ugurbil K, Elison JT, Zhang H, Shen D, Lin W (2023) Mapping the evolution of regional brain network efficiency and its association with cognitive abilities during the first twenty-eight months of life. Dev Cogn Neurosci 63:101284. https://doi.org/10.1016/j.dcn.2023.101284

Jones DK, Cercignani M (2010) Twenty-five pitfalls in the analysis of diffusion MRI data. NMR Biomed 23(7):803–820. https://doi.org/10.1002/nbm.1543

Krafnick AJ, Flowers DL, Luetje MM, Napoliello EM, Eden GF (2014) An investigation into the origin of anatomical differences in dyslexia. J Neurosci 34(3):901–908

Lampis V, Ventura R, Di Segni M, Marino C, D'Amato FR, Mascheretti S (2021) Animal models of developmental dyslexia: Where we are and what we are missing. Neurosci Biobehav Rev 131:1180–1197. https://doi.org/10.1016/j.neubiorev.2021.10.022

Landi N, Perdue M (2019) Neuroimaging genetics studies of specific reading disability and developmental language disorder: A review. Lang Linguist Compass 13(9):e12349. https://doi.org/10.1111/lnc3.12349

Lind PA, Luciano M, Wright MJ, Montgomery GW, Martin NG, Bates TC, Dyslexia, DCDC2 (2010) Normal variation in reading and spelling is associated with DCDC2 polymorphisms in an Australian population sample. Eur J Hum Genet 18(6):668–673. https://doi.org/10.1038/ejhg.2009.237

Litwińczuk MC, Muhlert N, Cloutman L, Trujillo-Barreto N, Woollams A (2022) Combination of structural and functional connectivity explains unique variation in specific domains of cognitive function. NeuroImage 262:119531. https://doi.org/10.1016/j.neuroimage.2022.119531

Livingstone MS, Rosen GD, Drislane FW, Galaburda AM (1991) Physiological and anatomical evidence for a magnocellular defect in developmental dyslexia. Proc Natl Acad Sci USA 88(18):7943–7947. https://doi.org/10.1073/pnas.88.18.7943

Lou C, Duan X, Altarelli I, Sweeney JA, Ramus F, Zhao J (2019) White matter network connectivity deficits in developmental dyslexia. Hum Brain Mapp 40(2):505–516. https://doi.org/10.1002/hbm.24390

Lyon GR, Shaywitz SE, Shaywitz BA (2003) A definition of dyslexia. Ann Dyslexia 53:1–14. https://doi.org/10.1007/s11881-003-0001-9

Maier-Hein KH, Neher PF, Houde JC et al (2017) The challenge of mapping the human connectome based on diffusion tractography. Nat Commun 8(1):1349. https://doi.org/10.1038/s41467-017-01285-x

Marino C, Meng H, Mascheretti S, Rusconi M, Cope N, Giorda R, Molteni M, Gruen JR (2012) DCDC2 genetic variants and susceptibility to developmental dyslexia. Psychiatr Genet 22(1):25–30. https://doi.org/10.1097/YPG.0b013e32834acdb2

Marino C, Scifo P, Della Rosa PA, Mascheretti S, Facoetti A, Lorusso ML, Giorda R, Consonni M, Falini A, Molteni M, Gruen JR, Perani D (2014) The DCDC2/intron 2 deletion and white matter disorganization: focus on developmental dyslexia. Cortex 57:227–243

Mascheretti S, De Luca A, Trezzi V et al (2017) Neurogenetics of developmental dyslexia: From genes to behavior through brain neuroimaging and cognitive and sensorial mechanisms. Transl Psychiatry 7:e987. https://doi.org/10.1038/tp.2016.240

Mascheretti S, Peruzzo D, Andreola C, Villa M, Ciceri T, Trezzi V, Marino C, Arrigoni F (2021) Selecting the most relevant brain regions to classify children with developmental dyslexia and typical readers using complex magnocellular stimuli and multiple kernel learning. Brain Sci 11(6):722. https://doi.org/10.3390/brainsci11060722

Mascheretti S, Arrigoni F, Toraldo A, Giubergia A, Andreola C, Villa M, Lampis V, Giorda R, Peruzzo D (2024) Alterations in neural activation in the ventral frontoparietal network during complex magnocellular stimuli in developmental dyslexia associated with READ1 deletion. Behav Brain Funct 20(1):16. https://doi.org/10.1186/s12993-024-00241-2

McGrath LM, Pennington BF, Shanahan MA, Santerre-Lemmon LE, Barnard HD, Willcutt EG, Defries JC, Olson RK (2011) A multiple deficit model of reading disability and attention-deficit/hyperactivity disorder: Searching for shared cognitive deficits. J Child Psychol Psychiatry 52(5):547–557

Meda SA, Gelernter J, Gruen JR, Calhoun VD, Meng H, Cope NA, Pearlson GD (2008) Polymorphism of DCDC2 reveals differences in cortical morphology of healthy individuals—a preliminary voxel based morphometry study. Brain Imaging Behav 2(1):21–26. https://doi.org/10.1007/s11682-007-9012-1

Meng H, Smith SD, Hager K, Held M, Liu J, Olson RK, Pennington BF, DeFries JC, Gelernter J, O'Reilly-Pol T, Somlo S, Skudlarski P, Shaywitz SE, Shaywitz BA, Marchione K, Wang Y, Paramasivam M, LoTurco JJ, Page GP, Gruen JR (2005) DCDC2 is associated with reading disability and modulates neuronal development in the brain. Proc Natl Acad Sci USA 102(47):17053–17058. https://doi.org/10.1073/pnas.0508591102

Meng H, Powers NR, Tang L, Cope NA, Zhang PX, Fuleihan R, Gibson C, Page GP, Gruen JR (2011) A dyslexia-associated variant in DCDC2 changes gene expression. Behav Genet 41(1):58–66. https://doi.org/10.1007/s10519-010-9408-3

Meskaldji DE, Vasung L, Romascano D, Thiran JP, Hagmann P, Morgenthaler S, Van De Ville D (2015) Improved statistical evaluation of group differences in connectomes by screening-filtering strategy with application to study maturation of brain connections between childhood and adolescence. NeuroImage 108:251–264. https://doi.org/10.1016/j.neuroimage.2014.11.059

Moreau D, Stonyer JE, McKay NS, Waldie KE (2018) No evidence for systematic white matter correlates of dyslexia: An activation likelihood estimation meta-analysis. Brain Res 1683:36–47. https://doi.org/10.1016/j.brainres.2018.01.014

Nobile M, Alberti B, Zuddas A (2007) CRS-R. Conners' Rating Scale—Revised. Organizzazioni Speciali, Firenze, Italy

Paloyelis Y, Rijsdijk F, Wood AC, Asherson P, Kuntsi J (2010) The genetic association between ADHD symptoms and reading difficulties: the role of inattentiveness and IQ. J Abnorm Child Psychol 38(8):1083–1095. https://doi.org/10.1007/s10802-010-9429-7

Paracchini S, Scerri T, Monaco AP (2007) The genetic lexicon of dyslexia. Annu Rev Genomics Hum Genet 8:57–79. https://doi.org/10.1146/annurev.genom.8.080706.092312

Pennington BF (2006) From single to multiple deficit models of developmental disorders. Cognition 101(2):385–413. https://doi.org/10.1016/j.cognition.2006.04.008

Perani D, Scifo P, Cicchini GM, Rosa PD, Banfi C, Mascheretti S, Falini A, Marino C, Morrone MC (2021) White matter deficits correlate with visual motion perception impairments in dyslexic carriers of the DCDC2 genetic risk variant. Exp Brain Res 239(9):2725–2740. https://doi.org/10.1007/s00221-021-06137-1

Peterson RL, Pennington BF (2015) Developmental dyslexia. Annu Rev Clin Psychol 11:283–307

Plourde V, Boivin M, Forget-Dubois N, Brendgen M, Vitaro F, Marino C, Tremblay RT, Dionne G (2015) Phenotypic and genetic associations between reading comprehension, decoding skills, and ADHD dimensions: evidence from two population-based studies. J Child Psychol Psychiatry 56(10):1074–1082. https://doi.org/10.1111/jcpp.12394

Powers NR, Eicher JD, Butter F, Kong Y, Miller LL, Ring SM, Mann M, Gruen JR (2013) Alleles of a polymorphic ETV6 binding site in DCDC2 confer risk of reading and language impairment. Am J Hum Genet 93(1):19–28. https://doi.org/10.1016/j.ajhg.2013.05.008

Powers NR, Eicher JD, Miller LL, Kong Y, Smith SD, Pennington BF, Willcutt EG, Olson RK, Ring SM, Gruen JR (2016) The regulatory element READ1 epistatically influences reading and language, with both deleterious and protective alleles. J Med Genet 53(3):163–171. https://doi.org/10.1136/jmedgenet-2015-103418

Ramus F, Altarelli I, Jednoróg K, Zhao J, Scotto di Covella L (2018) Neuroanatomy of developmental dyslexia: Pitfalls and promise. Neurosci Biobehav Rev 84:434–452. https://doi.org/10.1016/j.neubiorev.2017.08.001

Rauland A, Meisler SL, Alexander-Bloch AF, Bagautdinova J, Baller EB, Gur RE, Gur RC, Luo AC, Moore TM, Popovych OV, Reetz K, Roalf DR, Shinohara RT, Sotardi S, Sydnor VJ, Vossough A, Eickhoff SB, Cieslak M, Satterthwaite TD (2025) White matter bundle reconstruction from single-shell diffusion magnetic resonance imaging: Test-retest reliability and predictive capability across orientation distribution function reconstruction methods. Hum Brain Mapp 46(17):e70429. https://doi.org/10.1002/hbm.70429

Rimrodt SL, Peterson DJ, Denckla MB, Kaufmann WE, Cutting LE (2010) White matter microstructural differences linked to left perisylvian language network in children with dyslexia. Cortex 46:739–749

RivaV, Marino C, Giorda R, Molteni M, Nobile M (2015) The role of DCDC2 genetic variants and low socioeconomic status in vulnerability to attention problems. Eur Child Adolesc Psychiatry 24(3):309–318. https://doi.org/10.1007/s00787-014-0580-5

Riva V, Mozzi A, Forni D, Trezzi V, Giorda R, Riva S, Villa M, Sironi M, Cagliani R, Mascheretti S (2019) The influence of DCDC2 risk genetic variants on reading: Testing main and haplotypic

effects. Neuropsychologia 130:52–58. https://doi.org/10.1016/j.neuropsychologia.2018.05.021
Rosenberg J, Pennington BF, Willcutt EG, Olson RK (2012) Gene by environment interactions influencing reading disability and the inattentive symptom dimension of attention deficit/hyperactivity disorder. J Child Psychol Psychiatry 53(3):243–251. https://doi.org/10.1111/j.1469-7610.2011.02452.x
Rubinov M, Sporns O (2010) Complex network measures of brain connectivity: Uses and interpretations. NeuroImage 52(3):1059–1069. https://doi.org/10.1016/j.neuroimage.2009.10.003
Sartori G, Job R, Tressoldi PE (1995) Batteria per la Valutazione della Dislessia e della Disortografia Evolutiva. Organizzazioni Speciali, Firenze, Italy
Sartori G, Job R, Tressoldi PE (2007) DDE-2, Batteria per la Valutazione della Dislessia e della Disortografia Evolutiva-2
Scerri TS, Schulte-Körne G (2010) Genetics of developmental dyslexia. Eur Child Adolesc Psychiatry 19(3):179–197. https://doi.org/10.1007/s00787-009-0081-0
Scerri TS, Macpherson E, Martinelli A, Wa WC, Monaco AP, Stein J, Zheng M, Suk-Han Ho C, McBride C, Snowling M, Hulme C, Hayiou-Thomas ME, Waye MMY, Talcott JB, Paracchini S (2017) The DCDC2 deletion is not a risk factor for dyslexia. Transl Psychiatry 7(7):e1182. https://doi.org/10.1038/tp.2017.151
Schilling KG, Blaber J, Huo Y, Newton A, Hansen C, Nath V, Shafer AT, Williams O, Resnick SM, Rogers B, Anderson AW, Landman BA (2019) Synthesized b0 for diffusion distortion correction (Synb0-DisCo). Magn Reson Imaging 64:62–70. https://doi.org/10.1016/j.mri.2019.05.008
Škoch A, Rehák Bučková B, Mareš J et al (2022) Human brain structural connectivity matrices—ready for modelling. Sci Data 9:486. https://doi.org/10.1038/s41597-022-01596-9
Smith RE, Tournier JD, Calamante F, Connelly A (2012) Anatomically constrained tractography: Improved diffusion MRI streamlines tractography through effective use of anatomical information. NeuroImage 62(3):1924–1938. https://doi.org/10.1016/j.neuroimage.2012.06.005
Smith RE, Tournier JD, Calamante F, Connelly A (2015) SIFT2: Enabling dense quantitative assessment of brain white matter connectivity using streamlines tractography. NeuroImage 119:338–351
Stanley ML, Simpson SL, Dagenbach D, Lyday RG, Burdette JH, Laurienti PJ (2015) Changes in brain network efficiency and working memory performance in aging. PLoS ONE 10(4):e0123950. https://doi.org/10.1371/journal.pone.0123950
Stein J (2001) The magnocellular theory of developmental dyslexia. Dyslexia 7(1):12–36. https://doi.org/10.1002/dys.186
Stein J (2014) Dyslexia: the role of vision and visual attention. Curr Dev Disord Rep 1(4):267–280
Stein J, Talcott JB (1999) Impaired neuronal timing in developmental dyslexia: The magnocellular hypothesis. Dyslexia 5(2):59–77. https://doi.org/10.1002/(SICI)1099-0909(199906)5%3A2%253C59%3A%3AAID-DYS134%3E3.0.CO%3B2-F
Stein J, Walsh V (1997) To see but not to read: The magnocellular theory of dyslexia. Trends Neurosci 20(4):147–152. https://doi.org/10.1016/S0166-2236(96)01005-3
Tahedl M (2020) B.A.T.M.A.N: Basic and Advanced Tractography with MRtrix for All Neurophiles. https://doi.org/10.17605/OSF.IO/FKYHT
Tahedl M, Tournier JD, Smith RE (2025) Structural connectome construction using constrained spherical deconvolution in multi-shell diffusion-weighted magnetic resonance imaging. Nat Protoc 20(9):2652–2684. https://doi.org/10.1038/s41596-024-01129-1
Tournier JD, Smith R, Raffelt D et al (2019) MRtrix3: A fast, flexible and open software framework for medical image processing and visualisation. NeuroImage 202:116137. https://doi.org/10.1016/j.neuroimage.2019.116137
Tressoldi PE, Brembati F, Donini R, Iozzino R, Vio C (2012) Treatment of Dyslexia in a Regular Orthography: Efficacy and Efficiency (Cost-Effectiveness) Comparison Between Home vs Clinic-Based Treatments. Eur J Psychol 8:375–390
Tustison NJ, Avants BB, Cook PA, Zheng Y, Egan A, Yushkevich PA, Gee JC (2010) N4ITK: Improved N3 bias correction. IEEE Trans Med Imaging 29(6):1310–1320. https://doi.org/10.1109/TMI.2010.2046908
Vandermosten M, Boets B, Wouters J, Ghesquière P (2012) A qualitative and quantitative review of diffusion tensor imaging studies in reading and dyslexia. Neurosci Biobehav Rev 36(6):1532–1552. https://doi.org/10.1016/j.neubiorev.2012.04.002
Wechsler D (2006) Wechsler Intelligence Scale for Children, 3rd edn. Organizzazioni Speciali, Firenze, Italy
Wilcke A, Weissfuss J, Kirsten H, Wolfram G, Boltze J, Ahnert P (2009) The role of gene DCDC2 in German dyslexics. Ann Dyslexia 59(1):1–11. https://doi.org/10.1007/s11881-008-0020-7
Willcutt EG, Pennington BF, Duncan L, Smith SD, Keenan JM, Wadsworth S, Defries JC, Olson RK (2010) Understanding the complex etiologies of developmental disorders: behavioral and molecular genetic approaches. J Dev Behav Pediatr 31(7):533–544. https://doi.org/10.1097/DBP.0b013e3181ef42a1
Xu J, Yin X, Ge H, Han Y, Pang Z, Tang Y, Liu B, Liu S (2015) Attentional performance is correlated with the local regional efficiency of intrinsic brain networks. Front Behav Neurosci 9:200. https://doi.org/10.3389/fnbeh.2015.00200
Zhao J, Zhao Y, Song Z, Liu J, Thiebaut de Schotten M, Ramus F (2024) A decade of white matter connectivity studies in developmental dyslexia. Psychoradiology 4:kkae029. https://doi.org/10.1093/psyrad/kkae029
Zhong R, Yang B, Tang H, Zou L, Song R, Zhu LQ, Miao X (2013) Meta-analysis of the association between DCDC2 polymorphisms and risk of dyslexia. Mol Neurobiol 47(1):435–442. https://doi.org/10.1007/s12035-012-8381-7